様式第６号（第１０条関係）

鳥取県環境学術研究等振興事業費補助金研究実績報告書（環境創造部門）

研究期間（３年目/３年間）

研　究　者 又は 研究代表者	氏　　名	（ふりがな）り　　さんそく 李　　相錫
	所属研究機関 部局・職	鳥取大学大学院工学研究科・教授 電話番号　０８５７－３１－５９６１ 電子ﾒｰﾙ sslee@eecs.tottori-u.ac.jp
研究課題名	湖沼の水質モニタリング用MEMSセンサとユビキタスセンサネットワークシステムの開発	
研究結果	・樹脂を構造体と接着剤とする新しいpHセンサを試作できた。動作確認を行った結果、改善が必要であることがわかった。 ・開発中のpHセンサと集積化が可能なBODセンサとして湖沼に存在する電流生成菌を用いる方法を提案し、有機物量と電流生成量の関係を導くため基礎実験を行った。その結果、有機物量と電流生成菌の電流生成量とは相関があることがわかった。 ・pHセンサ、クロロフィルセンサ、濁度センサの集積化に向けたマイクロ流体デバイスの構造設計を行った。 ・センサノードの電源として発電デバイスを検討した結果、温度差を利用する発電方式が最も適していることがわかった。また高温部と低温部との距離がメータオーダーで離れている状況での温度差発電には新しい材料の検討が必要であることが明らかになった。 ・無線センサネットワークのノード筐体の改善を行い、再設計をし、システムの実現可能性を見極めるため試作を行った。	
研究成果	・樹脂を構造体と接着剤とする新しいpHセンサの作製技術が確立できた。樹脂の硬化条件の最適化は必要であるが、マイクロ流体デバイスとしての動作確認はできた。 ・設計・作製した無線センサネットワークシステムのノードは湖沼水でも問題なく動作できることが確認でき（システムとしての動作確認と筐体の水耐性に対する確認）、応用可能性が実証できた。 ・湖沼に存在する電流生成菌を用いる新しいBODセンサは有効であることが検証できた。 ・pHセンサ、クロロフィルセンサ、濁度センサなどを集積化したマイクロ流体デバイスの構造設計ができた。 ・温度差を利用する新しい発電素子の提案ができた。 ・無線センサネットワークシステムに関する研究成果の一部を国際会議で発表した。また濁度センサとクロロフィルセンサに関する研究成果を学術雑誌と国際会議で発表した。	
次年度研究計画	・本年度は最終年である。	
報告責任者	所属・職 氏名	鳥取大学 研究推進部 研究推進課 研究助成係　高田 志保 電話番号　0857-31-5494 電子ﾒｰﾙ　ken-jyosei@ml.adm.tottori-u.ac.jp

注１）表題には、環境部門、地域部門、北東アジア学術交流部門のいずれかを記載すること。
２）「研究期間（　　年目/　　年間））」及び「次年度研究計画」は、環境部門のみ記載すること。
３）研究者の知的財産権などに関する内容等で、非公開としたい部分は、罫線で囲うなど明確にし、その理由を記すこと。
４）研究実績のサマリーを併せて提出すること。

A Wireless Sensor Network Platform for Water Quality Monitoring

Tomoaki Kageyama[1], Masashi Miura[1], Akihiro Maeda[2], Akihiro Mori[2] and Sang-Seok Lee[1]
[1]Graduate school of Engineering, Tottori University, Tottori, Japan
[2]Environment Sanitation Research Center, Tohaku-gun, Tottori, Japan
tkageyama@turip.jp, sslee@ele.tottori-u.ac.jp

Abstract—**We have developing a wireless sensor network system for water quality monitoring. It consists of various sensors for the sensing of physical and chemical properties of water, and systems including wireless communication module, power module and interface between sensors and wireless communication module. In this paper, we report the development results of a novel wireless sensor network platform for water quality monitoring, which is proposed for rapid prototyping of wireless sensor network system. In order to demonstrate our novel wireless sensor network platform, we fabricated the platform as a sensor node and field-tested it with several sensors in the lake. As a result, we could confirm that our proposed novel platform was operated successfully in real environment.**

Keywords—wireless sensor network; platform; sensor node; water quality monitoring; protocol; field-test

I. INTRODUCTION

The natural water resources monitoring is important issue especially from the viewpoint of environment preservation and human health care. As a water monitoring method, a wireless sensor network (WSN) system is considered as a proper and effective one, because we can obtain the real time and over the wide area monitoring data through the WSN system. Currently, the main components of WSN system such as sensors and wireless communication modules are small and cheap, by which tremendous sensor nodes can be easily implemented. It makes precise and accurate water quality monitoring, and also a step towards the trillion sensor era.

We have developing a WSN system to monitor the natural water resources quality. It consists of sensors for the sensing of physical and chemical properties of water, and systems including wireless communication module, power module and interface between sensors and wireless communication module. Until now, as sensors for water quality monitoring, we have developed the pH sensor [1] and the turbidity sensor [2]. Other sensors such as chlorophyll sensor, BOD sensor and temperature sensor are under developing at present. Moreover, we have also developed a novel WSN platform to achieve complete WSN system for water quality monitoring, which is originally proposed for rapid prototyping of a WSN system. In this paper, we report the development results of our proposed WSN platform including its design, fabrication and field-test results.

II. DESIGN OF WSN PLATFORM

Sensors under development for a new application such as water quality monitoring systems are immature, not optimized for use and frequently replaced for test, while the sensors are utilized in the generic devices such as smartphones are well optimized. Therefore, it is necessary to develop a new WSN platform flexible to arbitrary various sensors for water quality monitoring. In the development of such flexible WSN platform integrating various sensors, the most important issue is the communication protocol. There are many wireless communication protocols for the sensor node [3]. Currently, as communication protocols, GPIB and USB protocols are popular and often used in many research fields. However, GPIB is not suitable for small devices in terms of size although it is robust. Moreover, USB is complicated and not easy to handle. Here, we propose a simple internal protocol used within a sensor node for the flexible WSN platform. Details are described as follows.

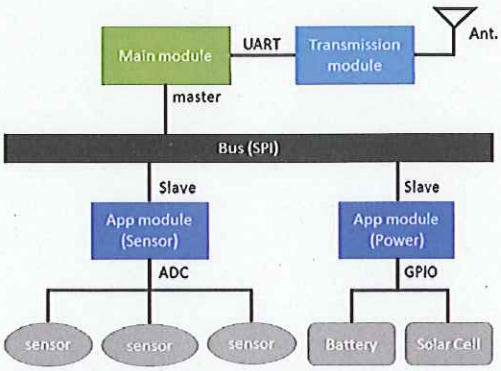

Fig. 1. Block diagram of system bus of our wireless sensor network platform. Main module is connected to the SPI bus as a master and the application modules are also connected to the SPI as a slave. Communication module and master are connected by an UART. An antenna is attached to the communication module. Application modules have sensors and power devices .

A. Bus

The bus structure of the WSN platform is shown in Fig. 1. The system consists of master, slave and communication modules. The main module (master module) manages other modules. Application modules have their own functions, which are connected to the main module through the serial peripheral interface (SPI). The main module behaves as an SPI master. By using the SPI, we don't need complicated address setting, which is easily available because it is implemented in most of

978-1-4799-8287-5/16/$31.00 ©2016 IEEE

<Top view>

PinNo.	Description
1	MISO
2	Vcc
3	SCK
4	MOSI
5	SS
6	GND

Fig. 2. Pin assignment of the connector. The top view of the connector mounted on the board is shown in the left. The pin assignment is based on the ICSP, however, the RESET pin has been assigned to the SS pin in our design.

the microcontrollers. The main module is connected to the transmission module for the communication as well through the universal asynchronous receiver transmitter (UART). Moreover, an antenna is attached to the transmission module. Application modules in our WSN platform consist of sensors for water quality monitoring and power devices for power sources such as battery and solar cell. The connection was implemented based on in-circuit serial programming (ICSP), and the box pin header (6-pin) was used as the connector. The pin assignment is summarized in Fig. 2. The difference between usual ICSP and used in ours is that slave select (SS) pin is assigned instead of RESET pin. As a result, by the switching of connection, it can be shared with the programming terminal to the microcomputer, which causes the reduction of the system size and the manufacturing cost.

B. Power

The power supply system is illustrated in Fig. 3. Power management is performed by the power management module which is one of the application modules. It generates 3.3 V through the DC/DC converter (TPS63060) for the Li-ion 1 cell battery, which supplies power to each circuit. Power management module has two 3.3 V power supply systems. One is the system for supplying power constantly, and another one is the system that can be operated ON/OFF by the instruction of the master module. Furthermore, the power can be supplied directly from the Li-ion cell battery, and the master module is capable of controlling it as well. Thereby, for the modules which do not need to be supplied constant power such as sensors module, even if it has not taken measures insufficiently to reduce power consumption, it is possible to reduce the adverse effect on the battery. Moreover, the power management module is also connected the solar panel to charge the Li-ion cell battery during the day. In order to improve the charging efficiency, the charging circuit LT3652 was used, which has the maximum power point tracking (MPPT) function. In the power module, the voltage monitoring system and the safety circuit are also implemented.

C. Transmission

Communication with the outside of the sensor nodes is performed with the Internet connection using the 3G mobile network. This makes it possible to observe the water quality monitoring results at any location where the Internet is available. We adopted the post method of https in data transmission to achieve the certification of encryption and server. However, it takes large power consumption when the

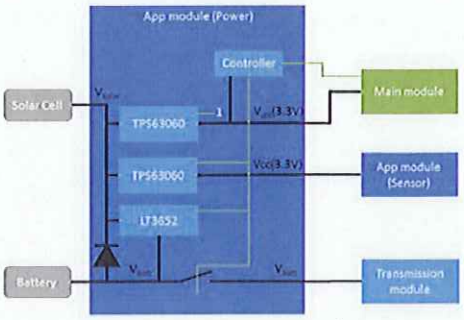

Fig. 3. Block diagram of the power supply system, which is simplified one to supply power to sensor node. Bold line and green colored line represent the power line and the control line, respectively. In the module, the voltage monitoring system and the safety circuit are implemented.

data are transmitted through the 3G network. If the power supply is limited, then it is necessary to perform the intermittent operation to save power consumption. In our prototyped WSN platform, the communication module is being powered directly from the Li-ion cell battery, which is performed by the master controller.

III. FABRICATION OF WSN PLATFORM

In order to demonstrate our designed WSN platform, we fabricated a sensor node using our WSN platform. Our sensor node is designed in a form of buoy to monitor the lake water quality.

The fabricated main module, power module and transmission module in the sensor node are shown in Fig. 4. Moreover, power sources such as Li-ion cell battery and solar cell are connected to the modules. For the detection with sensors, sensor circuit is connected further.

The sensor node was fabricated based on easily obtainable materials such as PVC pipe for the main frame, acrylic dome for the cover of assembled modules and Styrofoam for ensuring buoyancy. The transparent acrylic dome was utilized as the cover of module for the electric generation with solar cell during the day. The fabricated sensor node has the height of about 500 mm and the diameter of about 300 mm. The

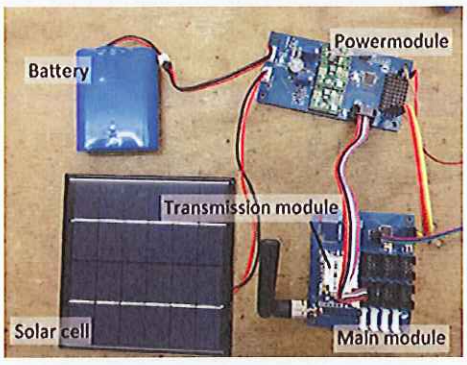

Fig. 4. The fabricated main module, power module (LT3652) and transmission module. The 6600mAh capacity Li-ion cell battery and solar cell are connected to power module.

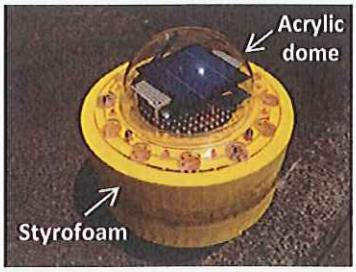

Fig. 5. The photograph of fabricated buoy type sensor node.

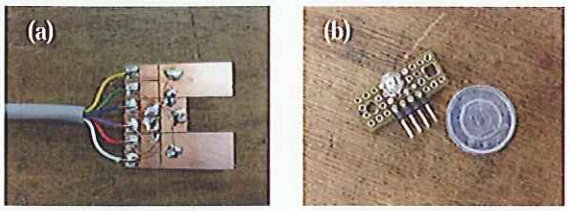

Fig. 6. The sensors utilized in field-test: (a) NTC thermistor and electrodes to measure electrical conductivity of the lake water and (b) temperature sensor and illuminometer.

photograph of fabricated buoy type sensor node is shown in Fig. 5.

IV. Field-Test of WSN Platform

We performed field-test to confirm the operation of our WSN platform using the fabricated sensor node shown in Fig. 5. In the test, temperature and electrical conductivity of the water were detected using negative temperature coefficient thermistor and in-house-made electrodes, which are shown in Fig. 6(a). The electrodes shown in Fig. 6(a) were implemented beneath the sensor node buoy and placed underwater. The circuit of the sensor was covered with silicone resin for waterproofing. Furthermore, we also implemented temperature sensor and illuminometer (Fig. 6(b)) in the acrylic dome to measure temperature and illuminance inside the acrylic dome.

The fabricated sensor node was placed on the lake as shown in Fig. 7 for the field-testing. The field-testing was performed for a week and the sensor node was operated without malfunction during the test. The measured data by

Fig. 7. The fabricated sensor node was placed on the lake Togo in Tottori prefecture, Japan for the field-testing.

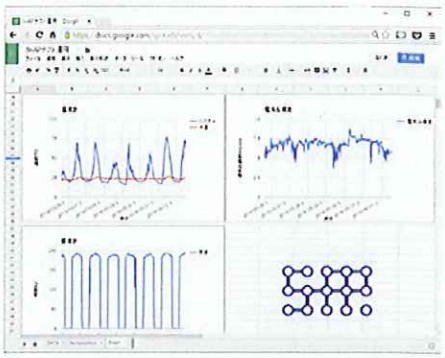

Fig. 8. A screen shot of a Google spreadsheet, in which the measurement results transmitted from the sensor node are displayed.

the sensors were transmitted every 10 minutes to server through the Internet connection using the 3G mobile network and the logged data are displayed on the Google spreadsheet. A screen shot of Google spreadsheet displaying measured and transmitted data in real time is shown in Fig. 8. In Fig. 8, water temperature and temperature in the dome, electrical conductivity of the water and illuminance are displayed in the left upper, right upper and left lower graphs, respectively as examples of acquired data. When performing data transmission, we powered on the module 1 minute prior to transmission, and we cut off the power after the data transmission to save the power.

V. Conclusions

We developed a novel WSN platform for water quality monitoring, which was proposed for rapid prototyping of WSN system. In order to demonstrate our novel WSN platform, we designed and fabricated the platform as a sensor node and field-tested it in the lake for a week with sensors such as temperature sensor, electrical conductivity sensor and illuminometer. As a result, we could obtain real time measured data transmitted from sensor node and confirm that our proposed novel platform was operated successfully in real environment. It means that our novel WSN platform using the proposed system is flexible, useful for rapid prototyping of a new WSN system and a low cost solution. Moreover, we believe that our WSN platform can be applied to not only water quality monitoring but also other various areas using WSN system.

References

[1] R. Komiyama, H. Miyashita, H. Okura, T. Kageyama, K. Ohmi, and S.-S. Lee, "A microfluidic device fully integrated with three pH sensing electrodes and passive mixer for nanoparticle synthesis", Proc. of IEEE Sensors 2015, Busan, Korea, pp. 1176-1179, Nov. 2015.

[2] R. Komiyama, T. Kageyama, M. Miura, H. Miyashita, and S.-S. Lee, "Turbidity monitoring of lake water by transmittance measurement with a simple optical setup", Proc. of IEEE Sensors 2015, Busan, Korea, pp. 1090-1093, Nov. 2015.

[3] J. Yick, B. Mukherjee, and D. Ghosal, "Wireless sensor network survey, " Computer Networks, vol. 52, pp. 2292-2330, Aug. 2008.

micromachines

MDPI

Article

A Feasibility Study on the Simultaneous Sensing of Turbidity and Chlorophyll *a* Concentration Using a Simple Optical Measurement Method

Ryota Isoyama [1], Manami Taie [1], Tomoaki Kageyama [1], Masashi Miura [1], Akihiro Maeda [2], Akihiro Mori [2] and Sang-Seok Lee [1,*]

1 Graduate School of Engineering, Tottori University, Tottori 680-8552, Japan; b13t3003@eecs.tottori-u.ac.jp (R.I.); b12t3032@faraday.ele.tottori-u.ac.jp (M.T.); m14t3010@faraday.ele.tottori-u.ac.jp (T.K.); contact@m-miura.jp (M.M.)

2 Environment Sanitation Research Center, Tottori 682-0704, Japan; maedaa@pref.tottori.lg.jp (A.Ma.); moriak@pref.tottori.lg.jp (A.Mo.)

* Correspondence: sslee@eecs.tottori-u.ac.jp; Tel.: +81-857-31-5961

Academic Editors: Wei Wang, Chia-Hung Chen, Zhigang Wu and Nam-Trung Nguyen
Received: 31 December 2016; Accepted: 23 March 2017; Published: 1 April 2017

Abstract: We have been developing a wireless sensor network system to monitor the quality of lake water in real time. It consists of a sensor module and a system module, which includes communication and power modules. We have focused on pH, turbidity and chlorophyll *a* concentration as the criteria for qualifying lake water quality. These parameters will be detected by a microfluidic device based sensor module embedded in the wireless sensor network system. In order to detect the turbidity and the chlorophyll *a* concentration simultaneously, we propose a simple optical measurement method using LED and photodiode in this paper. Before integrating a turbidity and chlorophyll *a* concentration sensor into the microfluidic device based pH sensor, we performed feasibility studies such as confirmation of the working principle and experiments using environmental water samples. As a result, we successfully verified our simultaneous sensing method by using a simple optical setup of the turbidity and the chlorophyll *a* concentration.

Keywords: water quality monitoring; turbidity; chlorophyll *a* concentration; optical setup; wireless sensor network

1. Introduction

In terms of natural resource preservation, a real-time and constant environmental monitoring system is an important research and development topic [1–6]. The targets of the environmental monitoring systems are very far-reaching and can include air, water, and soil. In this paper, we specifically focus on water quality monitoring, which is one of the most important issues worldwide. Water quality is closely related to the quality of drinking water and water for fishing and agriculture. In typical water quality monitoring systems, physical and chemical quantities such as pH, turbidity, dissolved oxygen concentration, chlorophyll *a* concentration, temperature, salinity, and pressure are monitored. However, a commercially available conventional water quality monitoring system is generally large and expensive. The high cost of monitoring systems prevents the real-time and continuous monitoring of a large area. In other words, sufficient numbers of water quality monitoring systems cannot be established in large natural resources such as lakes or rivers due to their high cost. It also causes low accuracy of water quality monitoring.

In order to obtain a low cost and high accuracy for lake or river water quality monitoring systems, we have been developing a wireless sensor network system. Our wireless sensor network system consists of a sensor module and a system module, which includes a wireless transceiver module,

control ICs for sensors, and a power module. Previous partial development results on the nodes of wireless sensor network systems have been reported in [7]. On the other hand, in the case of the sensor module, various sensors to monitor water quality, such as pH sensors, turbidity sensors, chlorophyll *a* concentration sensors, and temperature sensors, will be integrated into a microfluidic device. Among those sensors, we have developed a pH sensor. Our microfluidic device-based pH sensor measures pH with three electrodes: working, counter, and reference electrodes. We integrated three electrodes into the microfluidic channel, including a reference electrode. This can be applicable to not only water quality monitoring but also other fields such as nanoparticle synthesis monitoring [8]. Before integrating the turbidity and chlorophyll *a* concentration sensors into the microfluidic sensor module with a pH sensor, we studied the feasibility of simultaneous sensing through a simple optical measurement setup. Our optical measurement setup, using LEDs and photodiodes (PDs), is simple and costs little, whereas the commercial turbidity and chlorophyll *a* concentration sensors use expensive optical systems. Moreover, our measurement setup allows us to combine two sensors into one. Although many commercial turbidity and chlorophyll *a* concentration sensors require large samples or should directly contact samples due to their probe size or structure, respectively, our measurement setup does not require sample quantities that are as large, and we can detect turbidity and chlorophyll *a* concentration without contact. Our setup also provides more exact results in the calibration.

In this paper, we propose a simple optical measurement method for the simultaneous sensing of turbidity and chlorophyll *a* concentration, and report the results of a feasibility study.

2. Optical Measurement Setup

We propose a simple optical measurement method for the simultaneous sensing of turbidity and chlorophyll *a* concentration of the lake water. Basically, we obtain these two quantities with a single measurement setup by measuring the output light intensity, which is transmitted through the sample water. However, the physical origin of the output light to be detected is different when turbidity and chlorophyll *a* concentration measurements are taken. In the case of turbidity sensing, we detect the scattered light intensity caused from the suspended tiny pollutant particles in the water. In other words, the stronger the scattered light intensity is, the higher the degree of pollution will be. On the other hand, in the case of chlorophyll *a* concentration sensing, we detect the fluorescent light intensity emitted from chlorophyll *a* molecules. Chlorophyll *a* molecules emit fluorescence with a wavelength of around 685 nm when an excitation with a wavelength of around 450 nm is applied [9,10]. If the suspended aquatic phytoplankton is rich, then chlorophyll *a* concentration is high and the fluorescence intensity becomes strong.

A schematic diagram of the optical measurement setup is shown in Figure 1. In the optical measurement setup, we utilized low cost LEDs and photodiode (PD) as an incident light source and a detector of the transmitted light intensity, respectively. The small water sample bottle (diameter; 24 mm, height including lid; 52 mm) is put into the socket and fixed. The socket was fabricated by a 3D printing technique. As shown in Figure 1, in the socket, we prepared 5 holes for 2 LEDs and 3 PDs to investigate an optimal measurement position. However, generally, we use 2 LEDs such as a red and a blue LED. These 2 LEDs and 1 PD are sufficient to measure two quantities in real time.

In the experiment, we used the red LED with a typical wavelength of 624 nm (OS5RKA3131A, OptoSupply, Hong Kong, China) and the blue LED with a typical wavelength of 470 nm (OSB56A3131A, OptoSupply) as incident light for turbidity sensing and an excitation light for chlorophyll *a* fluorescence, respectively. The PD (S7183, Hamamatsu Photonics, Hamamatsu, Japan) with a spectral response range of 300–1000 nm was adopted. The diameter of the LEDs, and the area including the burr of the PD are 3 mm and 4.3×4.6 mm^2, respectively.

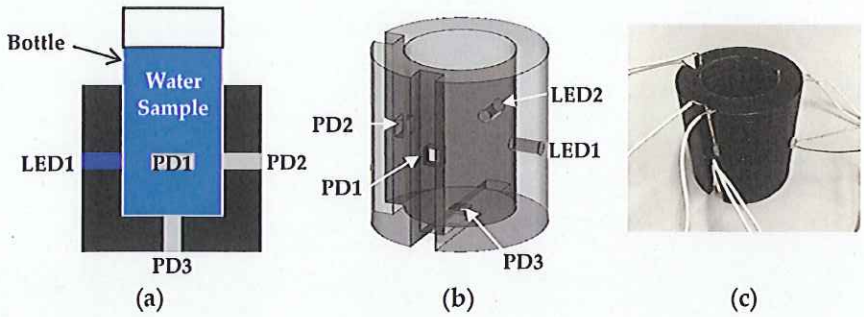

Figure 1. Optical measurement setup for turbidity and chlorophyll *a* concentration sensing: (**a**) schematic diagram of the optical measurement setup; (**b**) detailed structure of the socket; (**c**) photograph of a 3D printed socket with wires for measurement.

An equivalent circuit diagram of our optical measurement setup is shown in Figure 2. The power supply voltage (Vcc), the current control resistor (R1) for the LEDs, and the bias resistor (R2) for photovoltage measurement are 5 V, 0.984 kΩ, and 9.89 kΩ, respectively. In the experiment, a socket with the sample is placed in a box to prevent the influence of environmental light. A view of the experiment is shown in Figure 3. The measurement system is assembled based on the equivalent circuit shown in Figure 2. Moreover, in the experiment, we performed turbidity and chlorophyll *a* concentration sensing experiments individually to demonstrate feasibility.

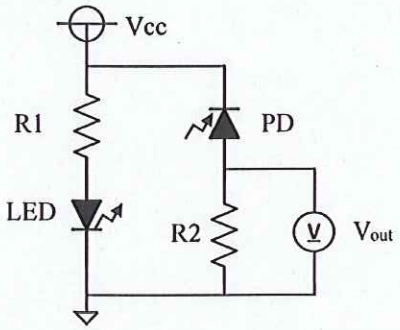

Figure 2. Equivalent circuit diagram of the optical measurement setup: The LED represents an LED1 or an LED2 in Figure 1b.

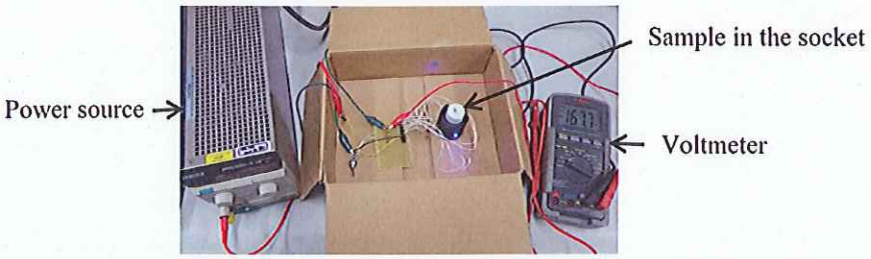

Figure 3. A view of the experiment with the optical measurement setup based on the circuit configuration shown in Figure 2.

3. Experiment Results and Discussions

We performed the turbidity and chlorophyll *a* concentration sensing experiments with standard samples for calibration and the environmental water samples to demonstrate the feasibility as follows, before performing the integration of two sensors into a microfluidic pH sensor.

3.1. Turbidity Sensing

Before the turbidity sensing experiment, we performed calibration to clarify the correlation between turbidities and output photovoltages. In accordance with international standard ISO 7027 [11], a formazine solution is recommended as the turbidity standard solution for measuring turbidity by the optical method. However, formazine is difficult to handle because a hydrazine sulfate, which is a carcinogenic agent, is necessary in the mixing process to obtain the formazine solution [12]. On the other hand, kaolin has been prevalently utilized as a turbidity standard solution for a long time. Since kaolin is a clay mineral, it is completely free of anything harmful, is easy to handle, and is a low-cost material. However, a kaolin solution settles easily. It causes variations in turbidity during the measurement. In order to resolve the problem, a styrene-divinylbenzene (St-DVB) copolymer microbeads solution was proposed as the turbidity standard solution. However, a St-DVB copolymer microbeads turbidity standard solution is much more expensive than other turbidity standard solutions. In the calibration, we utilized both a kaolin solution and a St-DVB copolymer microbeads solution.

First, we prepared 7 different concentration calibration solutions of kaolin. The prepared kaolin concentrations are 0, 10, 20, 50, 100, 200, and 500 mg/L, as shown in Figure 4. Then, we measured the photovoltages for each kaolin solution with the optical measurement setup shown in Figure 3. In the measurement, the red LED was set to the LED1 position in Figure 1b, and we measured the output photovoltages at three positions: PD1, PD2, and PD3, also shown in Figure 1b. The measurement results are represented in Figure 5. The photovoltages measured at the position of PD2 are not represented in Figure 5 because the position of PD2 is aligned with LED1 and because the photovoltages were out of range. In other words, PD2 measured the light intensity of the light source LED1 rather than that of the scattered light caused from the suspended kaolin particles. However, if the sample is a dense suspension or if the LED and PD are far away from each other, the measurement with LED1 and PD2 may also be valid.

As a result, we were able to distinguish the degrees of turbidity according to the measured photovoltages, but we could not distinguish them with the naked eye, especially for low concentration samples shown in Figure 4. Furthermore, we were also able to confirm the linear relationship between the concentration of the calibration solution and the scattered light intensity. The linearity was confirmed for the positions of both PD1 and PD3. We observed more accurate linearity in the measurement results from PD3. This linearity comes from the rapid precipitation effect of kaolin in the measurement, which means that the photovoltage measurement at the bottom of the sample yields a more accurate turbidity. Moreover, especially in low concentration regions of less than 50 mg/L, which is a region that is more meaningful for the sensors during detection, it shows better linearity. In turbidity sensing with environmental water samples, zero calibration is necessary only when the scattered light intensity is considered.

Figure 4. The 7 different concentration calibration solutions of kaolin: From left to right, the concentrations are 500, 200, 100, 50, 20, 10, and 0 mg/L.

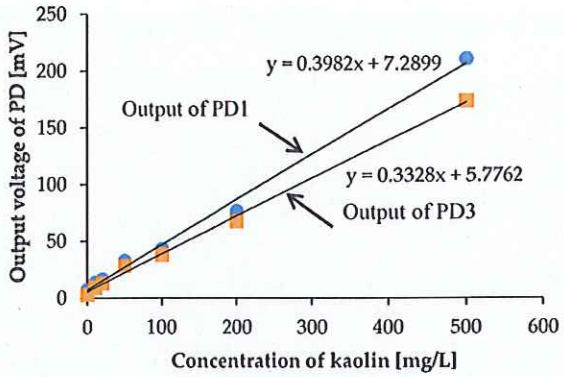

Figure 5. The measurement results for the calibration solutions of kaolin shown in Figure 4. PD1 is placed perpendicular to LED1, and PD3 is placed at the bottom of the sample.

To convert the photovoltage value to the Nephelometric Turbidity Unit (NTU), we measured the same kaolin calibration solutions with a commercial turbidity sensor (Hydrolab DS5X, OTT Hydromet GmbH, Kempten, Germany) calibrated with a formazine calibration solution. The NTU is defined by the formazine calibration solution. The turbidity measurement results are shown in Figure 6. Using the measurement results in Figure 6, the measured photovoltages were converted to NTU turbidities.

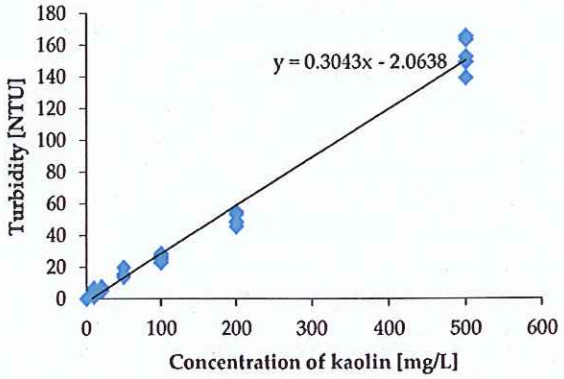

Figure 6. The measurement results by the commercial turbidity sensor for the same kaolin calibration solutions used in the measurement by the measurement setup in Figure 3. The photovoltage values can be converted to an NTU value.

We also performed turbidity measurements with environmental water samples from Lake Koyamaike located in the Tottori Prefecture of Japan. We collected eight measurement samples in Lake Koyamaike, and the places are indicated in Figure 7. Sample Nos. 3 and 4, and Nos. 5 and 6 were collected at the same place, but Sample Nos. 4 and 6 were collected after a pause. In the measurement, we measured the photovoltage for each sample, and it was converted to NTU turbidity using the relationship shown in Figure 6. The NTU turbidity measurement results are summarized in Figure 8. The photovoltage measurements were performed by PD1 and PD3, and the results were in agreement. The turbidity of Sample Nos. 4 and 5 are relatively higher than the others due to the muddiness of the stream during sampling.

No.	Coordinate
No.1	N35.50761 E134.17418
No.2	N35.49785 E134.15532
No.3-4	N35.49620, E134.15208
No.5-6	N35.50507 E134.12958
No.7	N35.51775 E134.15051
No.8	N35.52113 E134.16105

Figure 7. Sampling position at Lake Koyamaike in Tottori Prefecture, Japan. We collected 8 environmental water samples from Lake Koyamaike.

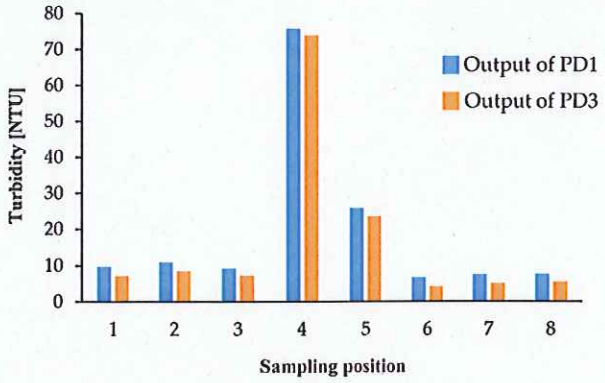

Figure 8. Turbidity measurement results for samples at the 8 places indicated in Figure 7.

We also performed calibration with the St-DVB copolymer microbeads solutions for comparison. For calibration solutions of St-DVB copolymer microbeads, we prepared eight different concentration calibration solutions. The prepared St-DVB copolymer microbeads solution concentrations were 0, 1, 2, 5, 10, 20, 50, and 100 mg/L and are shown in Figure 9. In the measurement, the measurement setup and procedure were the same as that used for the kaolin calibration solutions. The measurement results are shown in Figure 10. Here, we only measured the photovoltages from PD1 and PD3.

With the St-DVB copolymer microbeads calibration solution, we were also able to distinguish the degrees of turbidity according to the measured photovoltages. Moreover, we were able to successfully confirm the linear relationship between the concentration of the calibration solution and the scattered light intensity. Although the measurement results between PD1 and PD3 have small differences, we could obtain linearity with almost identical slopes. This means that the St-DVB copolymer microbeads are uniformly distributed in the solution and the precipitation effect can be ignored. The zero calibration is also necessary only to consider the scattered light intensity when we measure the turbidity of the environmental water sample.

Figure 9. The 8 different concentration calibration solutions of St-DVB copolymer microbeads: From left to right, the concentrations are 100, 50, 20, 10, 5, 2, 1, and 0 mg/L.

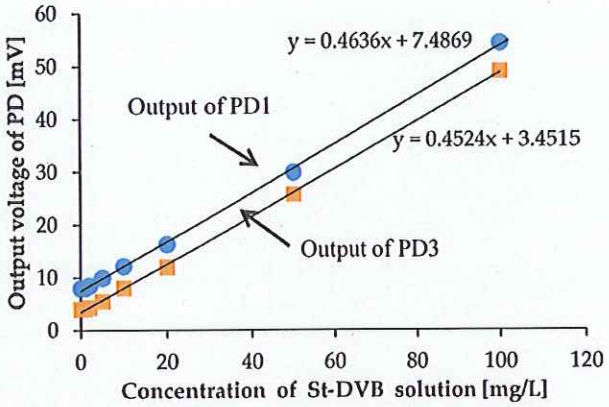

Figure 10. The measurement results for calibration solutions of St-DVB copolymer microbeads shown in Figure 9. PD1 is placed perpendicular to LED1, and PD3 is placed at the bottom of the sample.

We also performed turbidity measurements with the same environmental water samples, which were used in previous turbidity measurements. The measurement results based on the St-DVB copolymer microbeads solution calibration are shown in Figure 11. The NTU turbidity conversion was performed by using the relationship shown in Figure 6 as well. The turbidity values measured by PD1 agreed with those measured by PD3. Although the obtained turbidity values based on the St-DVB copolymer microbeads solution calibration were slightly smaller than those based on kaolin solution calibration. Specifically, in most low turbidity areas, the turbidity showed almost the same values. According to the measurement results for each calibration solution shown in Figures 5 and 10, the St-DVB copolymer microbeads solution calibration is considered as the more accurate method. However, in real applications, it is more important and meaningful to detect and clarify low turbidity water instead of high turbidity water. Therefore, the cheaper and easier method using the kaolin calibration solution is considered to be the effective one.

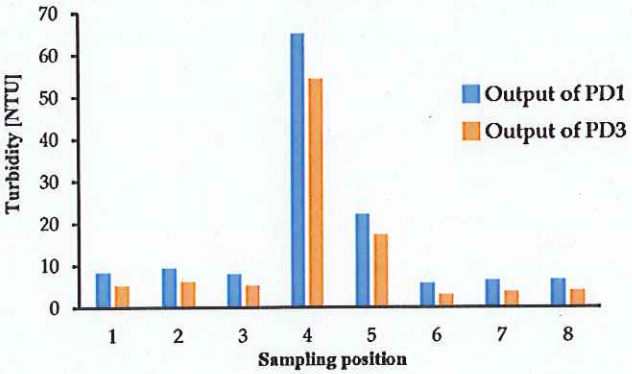

Figure 11. Turbidity measurement results based on St-DVB copolymer microbeads solution calibration for samples at the 8 places indicated in Figure 7.

3.2. *Chlorophyll* a *Concentration Sensing*

We also performed a chlorophyll *a* concentration sensing experiment with the same optical measurement setup shown in Figure 3. Before the measurement with an environmental water sample, we calibrated to clarify the correlation between chlorophyll *a* concentrations and output photovoltages. As calibration solutions of chlorophyll *a*, we prepared eight different concentration calibration solutions. The prepared chlorophyll *a* concentrations were 0, 5, 10, 20, 50, 100, 200, and 500 μg/L, which are shown in Figure 12. With the naked eye, the concentration differences cannot be distinguished. In the

measurement, the measurement setup and procedure are the same as what we used for the turbidity measurement, except for the LED. For chlorophyll *a* measurements, we utilized a blue LED instead of a red LED for the excitation of fluorescence. The blue LED was set to the LED2 position in Figure 1b. The measurement results are shown in Figure 13. In the measurement, the photovoltages were detected by PD3 only because detection by PD3 yielded better results in turbidity measurement. Moreover, we set a red filter sheet on PD3 to consider only the fluorescence around 685 nm in the measurement. For convenience in the red filter setup, we chose PD3 for the detection. As a result, we were also able to obtain good linearity between chlorophyll *a* concentrations and photovoltages. In other words, with the same simple optical measurement setup, we can easily detect both the turbidity and the chlorophyll *a* concentration. Commonly used commercial chlorophyll *a* sensors measure water soluble uranine (fluorescein disodium salt, $C_{20}H_{10}Na_2O_5$) fluorescence intensity for calibration, and measurement results are then converted to chlorophyll *a* concentration. However, by using our measurement setup, we can directly calibrate with the chlorophyll *a* that is dissolved in ethanol and diluted with water. In chlorophyll *a* concentration sensing with an environmental water sample, zero calibration is necessary to consider fluorescence intensity only.

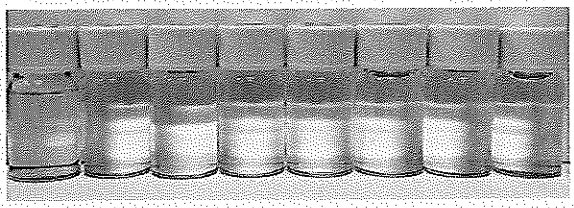

Figure 12. The 8 different concentration calibration solutions of chlorophyll *a*: From left to right, the concentrations are 500, 200, 100, 50, 20, 10, 5, and 0 μg/L.

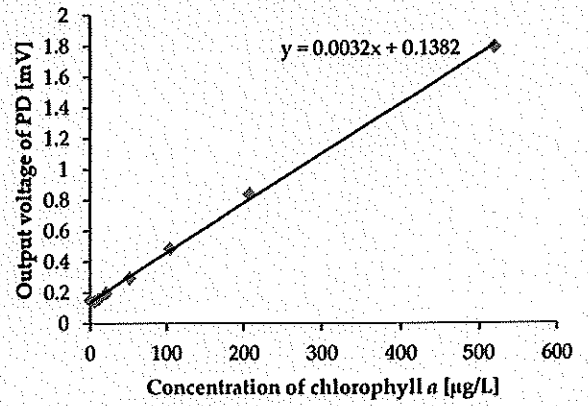

Figure 13. The measurement results for chlorophyll *a* solutions shown in Figure 12. PD3 placed at the bottom of the socket was used for detection.

We performed chlorophyll *a* concentration measurements with the same environmental water samples, which were used in previous turbidity measurements. The measured chlorophyll *a* concentrations are summarized in Figure 14. The chlorophyll *a* concentration was measured successfully with the same optical measurement setup applied to turbidity sensing. The chlorophyll *a* concentration is also one of the more important quantities in defining water quality. For instance, the turbidity of Sample No. 4 showed the highest value, but the chlorophyll *a* concentration of it was not high. This means that the environmental water sample at the Sample No. 4 position was only muddy and not polluted by phytoplankton.

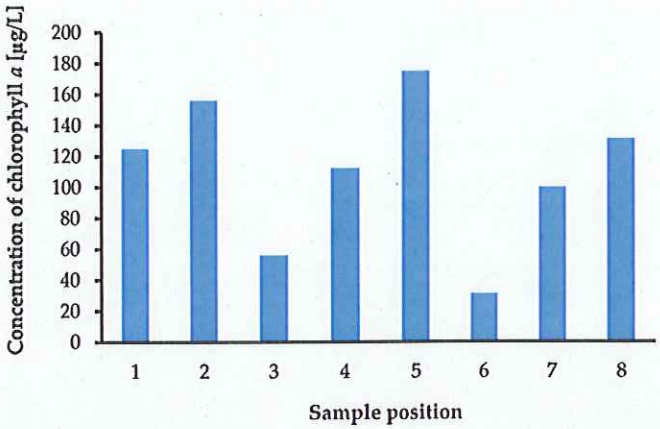

Figure 14. Chlorophyll *a* concentration measurement results for samples at the 8 places indicated in Figure 7.

In the chlorophyll *a* concentration measurement, we used a red filter in front of PD3 to effectively detect fluorescence. PD3 is also used for turbidity detection, and we performed the turbidity measurement again with a red filter on PD3 to investigate influence of the red filter installation on turbidity measurements. In the measurements, we measured photovoltages and NTU turbidities for kaolin calibration solutions shown in Figure 4 by using our measurement setup and a commercial sensor, respectively. The measurement results with and without the red filter on PD3 are shown in Figure 15. Although the output photovoltages are decreased due to scattered light intensity reduction for the high concentration sample, the linearity still exists; specifically, there are no remarkable variations for low concentration samples, which are samples that are more useful in real applications. As a result, it reveals that two LEDs and one PD are sufficient to simultaneously detect both the turbidity and chlorophyll *a* concentration with our measurement setup.

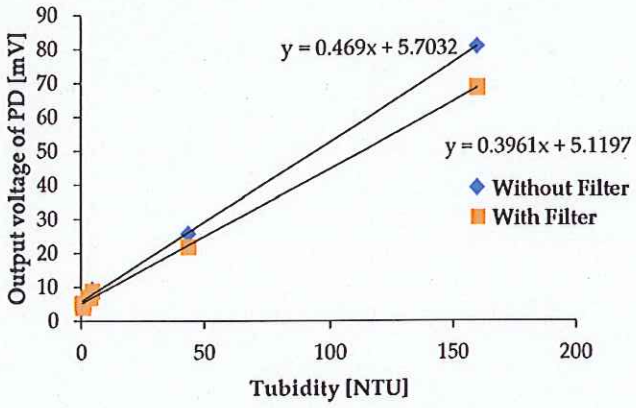

Figure 15. Comparison of the turbidity measurement results with and without a red filter on PD3.

In order to improve the strength of output photovoltages, we investigated the reflection effect of the socket. We put Al foil tape inside and around the socket to gather reflected scattered or fluorescent light to increase the output photovoltage. In the measurement, we used chlorophyll *a* solutions as samples shown in Figure 12. Moreover, a larger LED which has a 5 mm diameter was also tested. The measurement results are shown in Figure 16. Of course, all measurement results showed good linearity. There were no remarkable changes in the strength of photovoltages between 3 mm and 5 mm diameter LEDs. However, the output photovoltage strength was much more improved

when the reflective Al foil tape was applied. For instance, for the chlorophyll *a* concentration of the 5 µg/L sample, which is sample with the lowest concentration, the output photovoltage strength was increased by 14.9%. It is obvious that using reflection in the measurement setup is effective and should be considered when turbidity and chlorophyll *a* concentration sensors are integrated into a microfluidic sensor module, as shown in Figure 17.

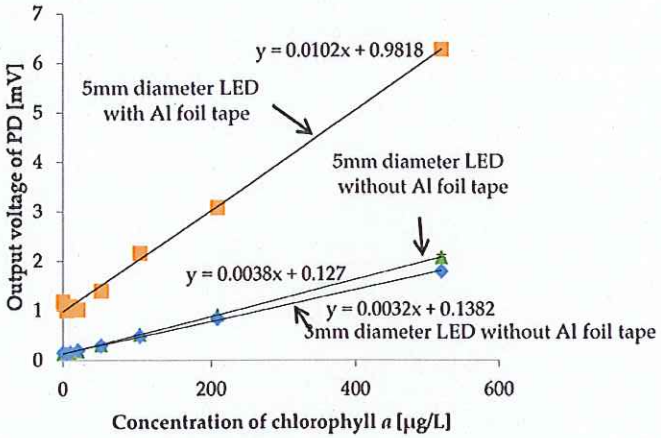

Figure 16. Comparison of the turbidity measurement results with and without a red filter on PD3.

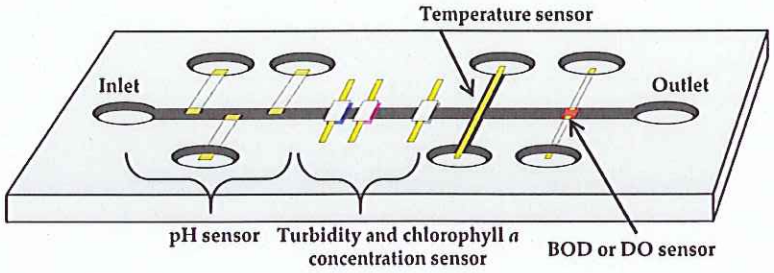

Figure 17. A schematic diagram of a microfluidic sensor module for the lake water quality monitoring wireless sensor network system.

In environmental water measurement, it is important to guarantee constant LED intensity. To do so, the ageing effect of LED intensity must be clarified, which will be considered as a follow-up to this work. Moreover, the intensity of the LEDs and the sensitivity of the PD should be optimized to obtain an optimal device size.

4. Conclusions

We have been developing a wireless sensor network system to monitor lake water quality in real time. It consists of a microfluidic sensor module and a system module. In this paper, we propose a simple optical measurement setup to detect turbidity and chlorophyll *a* concentration at the same time. Before integrating it into a microfluidic sensor module, we performed feasibility studies to confirm the working principle and to obtain guidance for an optimal device design.

In the feasibility study with the optical measurement setup, we investigated the turbidity and chlorophyll *a* sensing principles. We prepared calibration solutions for each sensing experiment, and performed measurements with them. As a result, we could confirm good linearity for both turbidity and chlorophyll *a* concentration sensing. Moreover, we performed measurements with environmental water samples and we could successfully distinguish the turbidity and chlorophyll *a* concentration

for each sample. Finally, the red filter effect on PD and the reflection effect of the socket were also investigated and clarified.

In the near future, turbidity and the chlorophyll *a* concentration sensors using an optical measurement setup will be integrated into microfluidics-based pH sensors.

Acknowledgments: The authors gratefully acknowledge the financial support provided to this study by the Tottori prefecture research fund for the promotion of environmental academic research.

Author Contributions: Sang-Seok Lee conceived and directed the project, and also contributed to the analysis and summarized the results. Ryota Isoyama, Manami Taie, Tomoaki Kageyama, and Masashi Miura prepared measurement setup and performed experiment. Akihiro Maeda and Akihiro Mori contributed to the measurement with commercial sensors and the analysis of measurement data. All authors commented on the paper.

Conflicts of Interest: The authors declare no conflict of interest.

References

1. Harvey, T.; Kratzer, S.; Philipson, P. Satellite-based water quality monitoring for improved spatial and temporal retrieval of chlorophyll-*a* in coastal waters. *Remote Sens. Environ.* **2015**, *158*, 417–430. [CrossRef]
2. Kiefer, I.; Odermatt, D.; Anneville, O.; Wuest, A.; Bouffard, D. Application of remote sensing for the optimization of in-situ sampling for monitoring of phytoplankton abundance in a large lake. *Sci. Total Environ.* **2015**, *527*, 493–506. [CrossRef] [PubMed]
3. Bhattacharjee, D.; Bera, R. Development of smart detachable wireless sensing system for environmental monitoring. *Int. J. Smart Sens. Intell. Syst.* **2014**, *7*, 1239–1253.
4. Wei, Q.; Nagi, R.; Sadeghi, K.; Feng, S.; Yan, E.; Ki, S.J.; Caire, R.; Tseng, D.; Ozcan, A. Detection and spatial mapping of mercury contamination in water samples using a smart-phone. *ACS Nano* **2014**, *8*, 1121–1129. [CrossRef] [PubMed]
5. Czugala, M.; Fay, C.; O'Connor, N.E.; Corcoran, B.; Benito-Lopez, F.; Diamond, D. Portable integrated microfluidic analytical platform. *Talanta* **2013**, *116*, 997–1004. [CrossRef] [PubMed]
6. Yu, K.S.; Gil, J.; Kim, J.; Kim, H.J.; Kim, K.; Park, D.; Kim, M.; Shin, H.; Lee, K.; Kwak, J.; et al. A miniaturized low-power wireless remote environmental monitoring system based on electrocheminal analysis. *Sens. Actuators B* **2014**, *102*, 27–34.
7. Kageyama, T.; Miura, M.; Maeda, A.; Mori, A.; Lee, S.-S. A wireless sensor network platform for water quality monitoring. *Proc. IEEE Sens.* **2016**, *2016*, 1442–1444.
8. Komiyama, R.; Miyashita, H.; Okura, H.; Kageyama, T.; Ishigaki, T.; Ohmi, K.; Lee, S.-S. A microfluidic device fully integrated with three pH sensing electrodes and passive mixer for nanoparticle synthesis. *Proc. IEEE Sens.* **2015**, *2015*, 1176–1179.
9. Krause, G.G.; Weis, E. Chlorophyll fluorescence and photosynthesis: The basics. *Annu. Rev. Plant Physiol.* **1991**, *42*, 313–349. [CrossRef]
10. Williamson, B.L.; Blondel, P.; Armstrong, E.; Bell, P.S.; Hall, C.; Waggitt, J.J.; Scott, B.E. A Self-Contained Subsea Platform for Acoustic Monitoring of the Environment around Marine Renewable Energy Devices–Field Deployments at Wave and Tidal Energy Sites in Orkney, Scotland. *IEEE J. Ocean Eng.* **2016**, *41*, 67–81.
11. ISO 7027-1:2016, Water Quality—Determination of Turbidity—Part 1: Quantitative Methods. Available online: http://www.iso.org/iso/catalogue_detail.htm?csnumber=62801 (accessed on 24 March 2017).
12. Muenzberg, M.; Hass, R.; Khanh, N.D.D.; Reich, O. Limitations of turbidity process probes and formazine as their calibration standard. *Anal. Bioanal. Chem.* **2017**, *409*, 719–728. [CrossRef] [PubMed]

A FEASIBILITY STUDY OF CHLOROPHYLL SENSOR USING A SIMPLE OPTICAL SETUP

M. Taie[1], T. Kageyama[1], A. Maeda[2], M. Mori[2], M. Miura[1] and S.-S. Lee[1]*
[1] Tottori University, Tottori, Japan
[2] Environment Sanitation Research Center, Tohaku-gun, Tottori, Japan

* Email: sslee@ele.tottori-u.ac.jp; Tel.: +81-(857) 31-5961

We are developing a wireless sensor network system to monitor water quality of natural water resources such as lake and river. A schematic view of the element of our wireless sensor network system is shown in Fig. 1, which consists of microfluidics based sensors, communication and power modules. As components of the microfluidics based sensor module, we have developed pH [1] and turbidity sensor [2]. Moreover, new sensors such as chlorophyll concentration sensor, temperature sensor and BOD sensor will be implemented. To do so, we performed a feasibility study to realize a microfluidics based chlorophyll concentration sensor and here we report the experiment results.

Our chlorophyll concentration sensor is realized with a simple optical setup using an LED and a photodiode (PD), which will be integrated with other sensors for water quality monitoring. It has advantage in terms of the integration of sensors since the simple optical setup for chlorophyll concentration sensing can be also applicable to turbidity sensing.

In order to verify chlorophyll concentration sensing with our optical setup before the integration, we performed feasibility study. To do so, we measured uranine (fluorescein disodium salt, $C_{20}H_{10}Na_2O_5$) fluorescence intensity in the experiment because commercial sensor is using the correlation between uranine. The fluorescence of uranine with the center wavelength of 521 nm for incident light with the center wavelength of 494 nm is shown in Fig. 2. In the experiment, we utilized 5 uranine solutions with different concentrations. The sample solutions are shown in Fig. 3 and the differences cannot be distinguishable by naked eyes.

Our experiment setup with the simple optical setup is described in Fig. 4. Each sample shown in Fig. 3 is contained in 10 mL glass bottle, which is fixed by a 3D printed socket. An LED and a PD are also attached on the socket. We measure photo-voltage of PD. The LED, we used, has emission peak at 470 nm. The PD has sensitivity from the range of 300 -1000 nm.

The experiment results by our simple optical setup and commercial sensor for the uranine samples are summarized in Fig. 5. The photo-voltages of fluorescence are measured at the bottom of socket. As a result, we obtained agreement on the measurement results between by our optical setup and by the commercial sensor.

Word Count <=377

Fig.1 A schematic diagram of the element of our wireless sensor network system to monitor the water quality.

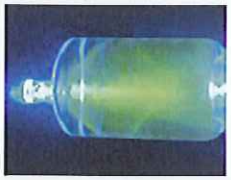

Fig. 2 Fluorescent image of uranine ($C_{20}H_{10}Na_2O_5$), which is used for the reference material of chlorophyll sensor.

Fig. 3 Uranine samples with different concentrations, which are not distinguishable each other by naked eyes.

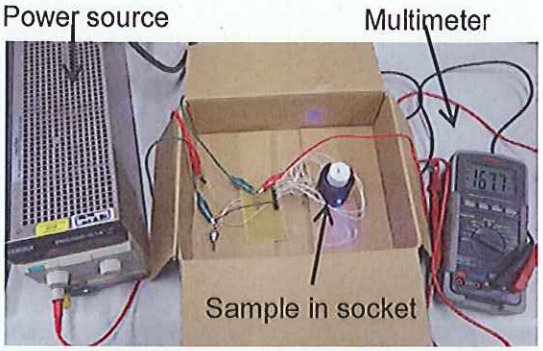

Fig. 4 Our simple optical measurement setup, which consists of power source, LED, photodiode, and multimeter.

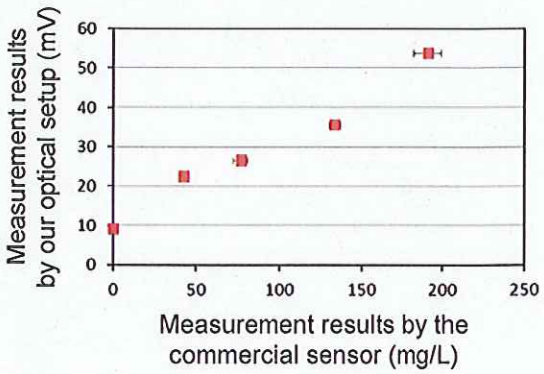

Fig. 5 Measurement results by our measurement setup and by the commercial sensor for uranine samples shown in Fig. 3.

REFERENCES:

[1] R. Komiyama, H. Miyashita, H. Okura, T. Ishigaki, T. Kageyama, K. Ohmi and S.-S. Lee, "Design and fabrication of a micro reactor integrated with pH electrodes and micro mixer for nanophosphor synthesis," Tech. Digest of the microTAS **2015**, 2035-2037.

[2] R. Komiyama, T. Kageyama, M. Miura, H. Miyashita and S.-S. Lee, "Turbidity monitoring of lake water by transmittance measurement with a simple optical setup," Proc. of IEEE Sensors **2015**, 1090-1093.